JOURNAL OF SPACECRAFT AND ROCKETS
Vol. 42, No. 3, May–June 2005

Method for Parking-Orbit Reorientation for Human Missions to Mars

Damon F. Landau* and James M. Longuski†
Purdue University, West Lafayette, Indiana 47907-2023
and
Paul A. Penzo‡
Global Aerospace Corporation, Altadena, California 91001-5327

Mars human-mission scenarios can incorporate a parking orbit at either Earth or Mars. In many cases the parking orbit is not conveniently oriented with respect to the interplanetary leg (e.g., returning to Earth from a parking orbit at Mars). A method to reorient the spacecraft's orbit around a planet for a roundtrip mission is described. This method includes a maneuver at apoapsis that rotates the parking orbit about the line of apsides to achieve the proper orientation at departure, thus coupling the effects of parking-orbit orientation with the interplanetary trajectories. We also account for the natural precession of the parking orbit during the stay time. The maneuver is most efficient for long period, eccentric orbits but can be used for any parking-orbit period or eccentricity. Moreover, this method often allows a significant range of orbital inclinations and can be modified to allow any desired inclination. The most significant drawback is the need to change the inclination at some point during the stay time. The reorientation maneuver can be applied to any set of arrival and departure interplanetary trajectories. We find that reorienting the parking orbit before departure can significantly reduce the total ΔV for many proposed missions.

Nomenclature

A	=	hyperbolic half-turn angle, deg
c	=	cosine
$\hat{\boldsymbol{h}}$	=	unit vector along angular momentum vector
n	=	mean motion, deg/s
R_P	=	planetary radius, km
$\boldsymbol{r}_p$	=	periapsis position vector, km
s	=	sine
$\boldsymbol{V}_{\text{apo}}$	=	velocity at apoapsis, km/s
$\boldsymbol{V}_\infty$	=	hyperbolic excess velocity, km/s
α	=	right ascension of $\boldsymbol{V}_\infty$, deg
α'	=	angle between arrival and departure $\boldsymbol{V}_\infty$, deg
β	=	B-plane angle, deg
ΔV	=	instantaneous change in velocity, km/s
δ	=	declination of $\boldsymbol{V}_\infty$, deg
μ	=	gravitational parameter, km^3/s^2
ϕ	=	rotation along line of apsides, deg

Subscripts

A	=	arrival
add	=	additional cost to include transfer geometry
D	=	departure
$3B$	=	perturbing third body

Introduction

IN many Mars mission designs, a vehicle is placed in a parking orbit. Generally, the orbit has the lowest periapsis and highest apoapsis practical to minimize the insertion and departure ΔV. Parking orbits reduce propulsion requirements because a smaller vehicle can then ferry the cargo and crew to and from the surface. A prime example is NASA's Design Reference Mission (DRM),[1] where the Earth return vehicle is placed in a highly elliptical Martian orbit. There are several other proposals that use parking orbits at Mars,[2,3] and some that incorporate parking orbits at both Earth and Mars.[4,5] To analyze the feasibility or effectiveness of the desired mission, we must estimate the ΔV cost of both placing the vehicle into the parking orbit and injecting to escape for the return trip. Often this cost is calculated as the sum of tangential burns at a common periapsis of the incoming/outgoing hyperbolic trajectory and the parking orbit (as in case 1, Fig. 1). However, this model does not account for the actual geometry of the transfer (as in case 2, Fig. 1), nor does it account for orbital precession caused by perturbing forces. Ignoring these effects will underestimate the departure mass at low-Earth orbit, sometimes by up to 50% (Refs. 6 and 7).

The only case where no additional mass is required occurs when the orbit precesses at exactly the right rate to align the orbit for a tangential periapsis burn at departure. This case, however, is rare[8,9] and often requires unacceptable transfer times and large ΔV. An effective method of reorienting a parking orbit to allow tangential maneuvers at periapsis for the general case was introduced by Luidens and Miller in 1966.[10] Their method involves rotating, or twisting, the parking orbit about the line of apsides via a maneuver at apoapsis, and was thus termed the "apo-twist." This maneuver, as we shall see, requires the alignment of the major axes, which is accomplished here by a judicious choice of the inclinations of the parking orbits at the times of arrival and departure. We present this method as an ideal component of interplanetary mission design, and we extend the previous work to account for orbital precession. We also include an alternate derivation of the apo-twist maneuver that is better suited for including perturbation effects. Performance characteristics are presented for current Mars mission proposals.

Problem

Figure 1 illustrates the problem of entering into and departing from a parking orbit by presenting an ideal situation (case 1) and a nonideal situation (case 2). Case 1 presents no difficulties because the planet provides sufficient bending to reach $\boldsymbol{V}_{\infty,D}$ with a tangential burn at periapsis. Here, the approach hyperbola, parking orbit,

Received 13 December 2003; revision received 23 April 2004; accepted for publication 26 April 2004.

*Graduate Student, School of Aeronautics and Astronautics; landau@ecn.purdue.edu. Student Member AIAA.

†Professor, School of Aeronautics and Astronautics, 315 N. Grant Street; longuski@ecn.purdue.edu. Associate Fellow AIAA.

‡Senior Engineer, 711 Woodbury Road, Suite H; paul.a.penzo@gaerospace.com. Associate Fellow AIAA.

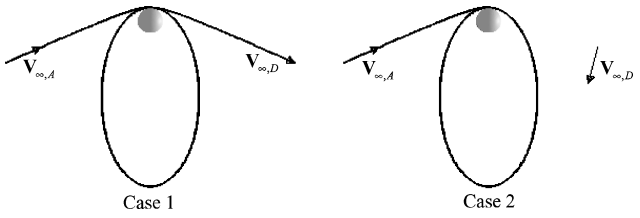

Fig. 1 Orientation of required V_∞ and parking orbit.

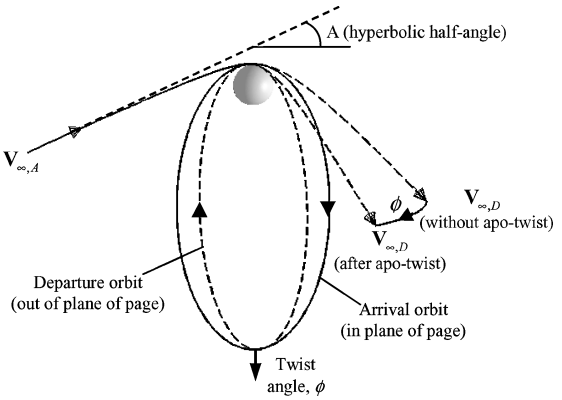

Fig. 2 Rotation of parking orbit about line of apsides by twist angle ϕ.

and departure hyperbola are coplanar and have the same periapsis. To calculate the ΔV (assuming conic trajectories), only the magnitudes of $\boldsymbol{V}_{\infty,A}$ and $\boldsymbol{V}_{\infty,D}$ are needed; the cost of entering the parking orbit is found explicitly via Eq. (1):

$$\Delta V_A = \sqrt{V_{\infty,A}^2 + 2\mu/r_p} - \sqrt{\mu(2/r_p - 1/a)} \qquad (1)$$

where r_p is the radius of periapsis and a is the semimajor axis of the parking orbit. The cost of departing is found by replacing $V_{\infty,A}$ with $V_{\infty,D}$.

To achieve $\boldsymbol{V}_{\infty,D}$ in case 2 seems difficult, but is possible with the apo-twist maneuver. In this case, $\boldsymbol{V}_{\infty,A}$, $\boldsymbol{V}_{\infty,D}$, and the parking orbit do not necessarily lie in the same plane. Even in the case where $\boldsymbol{V}_{\infty,A}$, and $\boldsymbol{V}_{\infty,D}$ are in the plane of the page, it will be necessary to target $\boldsymbol{V}_{\infty,A}$ so that the arrival parking orbit is not in the plane of the page. The selection of the arrival parking-orbit plane, combined with a maneuver at apoapsis (to rotate the departure parking orbit along the line of apsides), are the key ingredients of the apo-twist method. With this technique, the approach, parking orbit, and departure trajectories share a common periapsis, but the total ΔV will be greater than that provided by Eq. (1).

Proposed Method

If the parking orbit must be reoriented, then an ideal place to perform the reorientation maneuver is apoapsis because the velocity of the spacecraft is lowest at this point, and therefore relatively easy to change (i.e., with low ΔV), especially for highly eccentric obits. The period and eccentricity of the parking orbit are free parameters with the apo-twist method. To maintain its size and shape (a and e), the parking orbit is rotated along the line of apsides, that is, the arrival and departure parking orbits share a common periapsis and apoapsis. The greatest possible twist angle with the apo-twist maneuver is 180 deg, which can be achieved by a ΔV that is exactly twice the apoapsis velocity. For a fixed periapsis, as the period of the orbit increases, the magnitude of the apo-twist maneuver decreases. The apo-twist is illustrated in Fig. 2, where $\boldsymbol{V}_{\infty,A}$, the arrival orbit, and $\boldsymbol{V}_{\infty,D}$ (without apo-twist) are in the plane of the page. The desired $\boldsymbol{V}_{\infty,D}$ (which is out of the plane of the page) is achieved by rotating the parking orbit via the apo-twist maneuver.

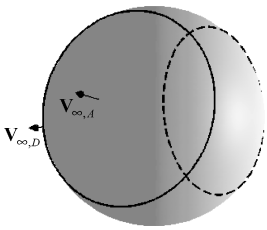

Fig. 3 Loci of periapses for ——, arrival and – – –, departure orbits.

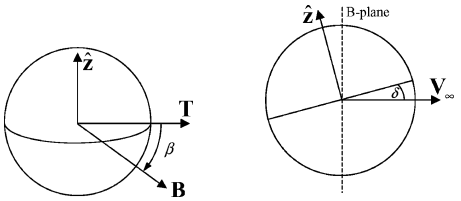

a) V_∞ into page at tip of B **b) T out of page with V_∞ at origin**

Fig. 4 Diagram of B-plane angle β.

Derivation of Equations

Analytic Solution for Keplerian-Orbit Model

To calculate an apo-twist maneuver, we begin by identifying all parking orbits that allow a tangential burn at periapsis. Figure 3 illustrates the locus of periapses for the arrival parking orbits (corresponding to $\boldsymbol{V}_{\infty,A}$) as a solid circle above the planet. Similarly, the dashed circle indicates the locus of periapses associated with the departure parking orbits and $\boldsymbol{V}_{\infty,D}$. We note that the circles are centered around and perpendicular to the $\boldsymbol{V}_\infty$. The arrival circle is on the same side of the planet as the direction of $\boldsymbol{V}_{\infty,A}$, and the departure circle is on the opposite side of $\boldsymbol{V}_{\infty,D}$ because the angle between the asymptote and periapsis of a hyperbola is always greater than 90 deg. The intersection of the solid and dashed circles indicates where an apo-twist maneuver can be used to rotate the arrival parking orbit to the orientation of the departure parking orbit.

Because the parking orbit and approach hyperbola share a common periapsis, the periapsis vector is readily computed by specifying the right ascension α and declination δ of $\boldsymbol{V}_\infty$, the hyperbolic half-angle A, and the B-plane angle β. The interplanetary trajectory specifies the arrival and departure $\boldsymbol{V}_\infty$, while the desired periapsis radius determines the hyperbolic half-angle, leaving the arrival and departure B-plane angles as free variables to choose the periapsis vector. The hyperbolic half-angle is illustrated in Fig. 2 and given by

$$A = \sin^{-1}\left[\mu \Big/ \left(\mu + V_\infty^2 r_p\right)\right], \qquad A \in [0, 90] \text{ deg} \qquad (2)$$

The B-plane is defined as a plane that passes through the center of the target planet, perpendicular to $\boldsymbol{V}_\infty$. Furthermore, the aimpoint is the intersection of $\boldsymbol{V}_\infty$ and the B plane, and the B-plane angle is measured clockwise from $\boldsymbol{T}$ ($\boldsymbol{T} \equiv \boldsymbol{V}_\infty \times \hat{\boldsymbol{z}}$) to $\boldsymbol{B}$ (the aimpoint). Thus, the B-plane angle specifies the direction of the aimpoint around the disc of the planet. It is assumed that any aimpoint can be achieved for virtually no propellant cost (provided the targeting maneuver is performed early enough in the approach trajectory). In Fig. 4a the B plane is the plane of the page, and the view direction is along $\boldsymbol{V}_\infty$. The $\hat{\boldsymbol{z}}$ axis is rotated out of the plane of the page forward through the declination δ, but both $\boldsymbol{T}$ and $\boldsymbol{B}$ are in the view plane. The curved line in Fig. 4a and the tilted line in Fig. 4b demarcate the intersection of the planet and a plane normal to $\hat{\boldsymbol{z}}$. For example, if $\hat{\boldsymbol{z}}$ is chosen to be the planet's spin axis, then these lines would trace the equator. Figure 4b offers a view opposite $\boldsymbol{T}$ and is included for clarity. (Also, the $\boldsymbol{V}_\infty$ is placed at the origin to illustrate δ.)

We calculate the orbital coordinate system ($\hat{\boldsymbol{r}}$, $\hat{\boldsymbol{\theta}}$, $\hat{\boldsymbol{h}}$) at periapsis through sequential rotations of α, δ, β, and A, defining the direction cosine matrix from orbital coordinates to inertial coordinates ($\hat{\boldsymbol{x}}$, $\hat{\boldsymbol{y}}$, $\hat{\boldsymbol{z}}$):

$$\begin{Bmatrix} \hat{\boldsymbol{x}} \\ \hat{\boldsymbol{y}} \\ \hat{\boldsymbol{z}} \end{Bmatrix} = \begin{bmatrix} c_\alpha c_\delta s_A + (s_\alpha c_\beta + c_\alpha s_\delta s_\beta) c_A & c_\alpha c_\delta c_A - (s_\alpha c_\beta + c_\alpha s_\delta s_\beta) s_A & s_\alpha s_\beta - c_\alpha s_\delta c_\beta \\ s_\alpha c_\delta s_A + (-c_\alpha c_\beta + s_\alpha s_\delta s_\beta) c_A & s_\alpha c_\delta c_A + (c_\alpha c_\beta - s_\alpha s_\delta s_\beta) s_A & -c_\alpha s_\beta - s_\alpha s_\delta c_\beta \\ s_\delta s_A - c_\delta s_\beta c_A & s_\delta c_A + c_\delta s_\beta s_A & c_\delta c_\beta \end{bmatrix} \begin{Bmatrix} \hat{\boldsymbol{r}} \\ \hat{\boldsymbol{\theta}} \\ \hat{\boldsymbol{h}} \end{Bmatrix} \tag{3}$$

For the departure periapsis, we replace A with $-A$.

To simplify the analysis of this matrix, we define $\hat{\boldsymbol{z}}$ to be perpendicular to the plane created by the incoming and outgoing $\boldsymbol{V}_\infty(\delta = 0)$, and the incoming $\boldsymbol{V}_\infty$ right ascension is rotated to zero. We apply these conditions because, at this point, no perturbations are modeled and the planet's orientation is not critical. These assumptions provide the following conditions.

Arrival:

$$\alpha = 0, \qquad \delta = 0, \qquad A = A_A, \qquad \beta = \beta_A \tag{4}$$

Departure:

$$\alpha = \alpha', \qquad \delta = 0, \qquad A = -A_D, \qquad \beta = \beta_D \tag{5}$$

where α' is the angle (between 0 deg and 180 deg) from $\boldsymbol{V}_{\infty,A}$ to $\boldsymbol{V}_{\infty,D}$. The size and shape of the parking orbit provides the magnitude of periapsis, while the first column of Eq. (3) gives the direction of periapsis in inertial coordinates. Thus for the arrival and departure orbits to share a common periapsis ($\boldsymbol{r}_{p,A} = \boldsymbol{r}_{p,D}$) the following conditions [from the first column of Eq. (3)] must be satisfied:

$$s_{A_A} = -c_{\alpha'} s_{A_D} + s_{\alpha'} c_{\beta_D} c_{A_D} \tag{6}$$

$$c_{\beta_A} c_{A_A} = s_{\alpha'} s_{A_D} + c_{\alpha'} c_{\beta_D} c_{A_D} \tag{7}$$

$$s_{\beta_A} c_{A_A} = s_{\beta_D} c_{A_D} \tag{8}$$

Equations (6) and (7) are combined to calculate the arrival and departure B-plane angles:

$$c_{\beta_D} = \frac{s_{A_A} + c_{\alpha'} s_{A_D}}{s_{\alpha'} c_{A_D}} \tag{9}$$

$$c_{\beta_A} = \frac{s_{A_D} + c_{\alpha'} s_{A_A}}{s_{\alpha'} c_{A_A}} \tag{10}$$

The positive or negative value for β_D can be chosen arbitrarily, but from Eq. (8) if β_A is positive then β_D must also be positive and vice versa. This combination of B-plane angles will ensure that the incoming and outgoing $\boldsymbol{V}_\infty$ can be achieved from the same periapsis, and an orbital maneuver is required only at apoapsis.

We calculate the reorientation cost as the ΔV for rotating the apoapsis velocity $\boldsymbol{V}_{\text{apo}}$ through a given angle ϕ:

$$\Delta V = 2 V_{\text{apo}} \sin(\phi/2) \tag{11}$$

The angle through which the orbit must rotate is the angle between the two angular momentum vectors, given by the third column of Eq. (3):

$$\hat{\boldsymbol{h}}_A = \begin{bmatrix} 0 \\ -s_{\beta_A} \\ c_{\beta_A} \end{bmatrix}, \qquad \hat{\boldsymbol{h}}_D = \begin{bmatrix} s_{\alpha'} s_{\beta_D} \\ -c_{\alpha'} s_{\beta_D} \\ c_{\beta_D} \end{bmatrix} \tag{12}$$

The reorientation angle ϕ is found by taking the dot product between these vectors:

$$c_\phi = \hat{\boldsymbol{h}}_A \cdot \hat{\boldsymbol{h}}_D = \frac{c_{\alpha'} + s_{A_A} s_{A_D}}{c_{A_A} c_{A_D}} \tag{13}$$

Thus, for a given set of α', A_A, and A_D, the location of the apo-twist maneuver is calculated using Eqs. (9) and (10), and the cost is provided by Eq. (11).

In general, there will be two possible locations to perform the apo-twist [principal and nonprincipal values of Eqs. (9) and (10)]. Geometrically, this occurs because the set of arrival and departure periapses form circles that rest on a sphere with a radius equal to the periapsis magnitude (as shown in Fig. 3). The intersections of these circles are locations where the arrival and departure parking orbits share common apses; thus, an apo-twist is possible.

If the planet provides just enough bending to reach $\boldsymbol{V}_{\infty,D}$, then the circles become tangent, and no apo-twist is required ($\phi = 0$ deg). However, as $\boldsymbol{V}_{\infty,A}$ and $\boldsymbol{V}_{\infty,D}$ become aligned (i.e., as $\alpha' \to 0$ deg) the circles will not intersect, and no apo-twists can occur. Similarly, as $\alpha' \to 180$ deg the circles will again become tangent at some point. In this case $\boldsymbol{V}_{\text{apo}}$ must be totally reversed, requiring the largest apo-twist maneuver ($\phi = 180$ deg). These special cases set the bounds on α':

$$A_A + A_D \le \alpha' \le 180\,\text{deg} - |A_D - A_A| \tag{14}$$

These bounds can also be verified by setting $\phi = 0$ or 180 deg in Eq. (13). Thus, when α' is too small or too large the apo-twist will not work (if no perturbations are present).

Solution Algorithm for Perturbed-Orbit Model

We choose a relatively simple perturbation model that includes only the secular changes in the ascending node Ω and argument of periapsis ω caused by oblateness J_2 and perturbing third bodies (the sun and moon at Earth and the sun at Mars). The corresponding angular rates are provided by Ref. 11:

$$\dot{\Omega}_{J_2} = -\frac{3}{2} n \frac{J_2 R_P^2}{a^2 (1 - e^2)^2} \cos i \tag{15}$$

$$\dot{\omega}_{J_2} = \frac{3}{4} n \frac{J_2 R_P^2}{a^2 (1 - e^2)^2} (4 - 5 \sin^2 i) \tag{16}$$

$$\dot{\Omega}_{3B} = -\frac{1}{f} \frac{3}{16} \frac{n_{3B}^2}{n} \frac{(2 + 3e^2) \cos i}{\sqrt{1 - e^2}} \left(3 \cos^2 i_{3B} - 1\right) \tag{17}$$

$$\dot{\omega}_{3B} = \frac{1}{f} \frac{3}{16} \frac{n_{3B}^2}{n} \frac{(4 - 5 \sin^2 i + e^2)}{\sqrt{1 - e^2}} \left(3 \cos^2 i_{3B} - 1\right) \tag{18}$$

In Eqs. (17) and (18), $f = 1$ for solar perturbations and $f = m_{\text{Earth}}/m_{\text{Moon}} \approx 81.3$ for lunar perturbations. We choose this model [Eqs. (15–18)] because it captures the main perturbation effects on large, elliptical orbits. A more accurate model would include a higher-order gravity field and variations in eccentricity and inclination. However, these effects are quite small compared to Eqs. (15–18) and are omitted to save computation time.

The effects of these perturbations on the apo-twist are shown at three different maneuver times in Fig. 5. (In the specific case of Fig. 5, we assume a mission where the crew departs Earth on 9 March 2016 and arrives at Mars on 5 October 2016. A vehicle is then placed in a parking orbit with a period of one day and a periapsis altitude of 300 km. After 531 days at Mars the crew departs on 20 March 2018 and arrives back at Earth on 16 October 2018.) In the absence of perturbations, the periapsis vector of any given parking orbit remains fixed. Thus in the case of Fig. 3, the time of the apo-twist maneuver has no effect in the application of the maneuver. However, when perturbations are considered, the periapsis vector will continue to move over the duration of the stay time. The effect of these perturbations can be thought of as a projection in time of the original periapses loci in Fig. 3. If an apo-twist maneuver is performed at the midpoint of the stay time then the arrival circle must be propagated forward in time, and the departure circle must be projected backwards in time to find intersections where the maneuver can be accomplished. The resulting contours of the propagated circular periapses loci are surprisingly complex. Figure 5b illustrates the perturbed loci to the middle of the stay time. In Fig. 5a, where

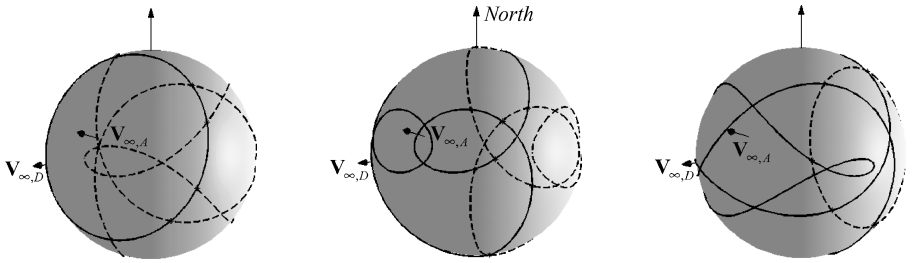

a) Arrival **b) Middle of stay time** **c) Departure**

Fig. 5 Loci of periapses for ——, arrival and – – –, departure orbits (with perturbations).

the apo-twist maneuver is performed at arrival, the arrival periapses locus is still a circle; however, the departure periapses will vary over the entire stay time and thus form an intricate curve. Figure 5c represents the departure time, so that the arrival orbits have been perturbed over the entire stay time, but the departure periapses have no time to vary and once again form the familiar circle. (We note that very few contours appear on the opposite side of the spheres in Fig. 5.) Because the perturbations can move the apoapsis position significantly during the course of the stay time, the restrictions from Eq. (14) often no longer apply, especially for long stay times (e.g., 500 days). So, cases where the apo-twist is not possible without perturbations can become possible when perturbations are present.

In fact, multiple apo-twist opportunities (locations where the arrival periapses locus intersects the departure periapses locus) often exist for a given maneuver time when perturbations are considered. For example, in Fig. 5 there are six, eight, and six possible apo-twist maneuvers at the beginning, middle, and end of the stay time, respectively. When the apo-twist maneuvers are considered as a function of time over the entire mission duration, the discrete apo-twist locations in Fig. 5 become the sets of lines indicated in Fig. 6. As an example, we consider the southernmost apo-twist location (solid and dashed intersection) in Fig. 5a. This apo-twist corresponds to the left end of the line near the south pole of Fig. 6. Similarly, the southern apo-twist in Fig. 5c marks the right end of this southernmost line in Fig. 6. The entire line is found by continuously varying the maneuver time (we choose one-day increments) from the arrival date to the departure date. We note that there are infinitely many possible apo-twist maneuvers when perturbations are considered (Fig. 6), which greatly contrasts the Keplerian orbit model (Fig. 3), in which there are, at most, two different apo-twist locations. The additional possibilities in the perturbation case introduce flexibility for designing human missions to Mars.

The process of calculating apo-twist maneuvers when orbit perturbations are present is similar to the no-perturbation case: we determine the conditions necessary for the arrival orbit and departure orbit to have the same apoapsis vector (and therefore the same periapsis vector), then calculate the angle ϕ between these orbits. The main difference is that the time of the maneuver provides an extra degree of freedom in the apo-twist solution. Because of the added complexity of including precession effects, we adopt a numerical approach to the problem. Our method is generalized by the following steps:

1) Calculate the set of arrival and departure orbits where a tangential periapsis burn is possible via Eq. (3) by varying β_A and β_D. This calculation provides the arrival (solid) and departure (dashed) circles of Fig. 3, where we choose to compute 360 orbits.

2) Determine the precession of the arrival orbits up to a given maneuver time with a perturbation model. Similarly, reverse the precession of the departure orbits from departure time back to the maneuver time. These precession effects create the complex contours in Fig. 5.

3) Select combinations of β_A and β_D such that the corresponding apoapsis vectors match (within a small tolerance) for the given maneuver time. This step is equivalent to locating the intersections in Fig. 5 (for the 360 orbits).

4) Use these β_A, β_D combinations as a starting point to drive the difference in arrival and departure apoapsis vectors to zero via a nonlinear equation solver. This step removes the remaining errors caused by starting with 360 discrete orbits.

5) Repeat steps 2–4 for different maneuver times until the parking orbit duration is sufficiently sampled (as in Fig. 6).

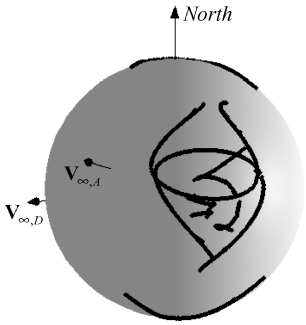

Fig. 6 All possible apo-twist maneuvers during the stay time.

Application of the Apo-Twist

We now examine a representative Mars mission scenario that employs parking orbits at both Earth and Mars to determine the effectiveness of the apo-twist.[4] This scenario corresponds well with many long stay-time (500–700 days) missions.[1–5,12] (We refer the reader to Ref. 13 for an application of the apo-twist to semicycler[2] and DRM-type[1,12] missions.) The parking orbit is assumed to have a period of one day and a periapsis altitude of 300 km. A parking orbit of this size and shape allows a relatively small arrival and departure maneuver and still stays well within the sphere of influence of both Mars and Earth.

The arrival and departure ΔV and orbital inclination drive the cost of the parking orbit (which must be considered in context of the entire mission). Other issues such as the lighting conditions at arrival and the available landing range can also affect the parking-orbit selection.[14] The ΔV indicates how much propellant is required to enter and depart the orbit, and the inclination determines how much propellant is needed to reach the surface. The inclination should be as close to the latitude of the launch/landing site as possible to make full use of the planet's rotation. But the arrival inclination is not as important, because the atmosphere might be used to reach the landing site with modest propellant expenditure (as long as the inclination is greater than the latitude of the site). If the mission involves rendezvous with a moon, then the parking-orbit inclination should be as close to the moon's inclination as possible. However, in many scenarios the interplanetary transport vehicle is much more massive than the launch/landing vehicle, and so the ΔV is usually weighted more than the inclination when minimizing propellant cost. Generally, low ΔV and prograde inclinations are desired, but the best combination is mission dependent.

To further assess the effectiveness of the apo-twist (which requires three burns), we compare it to a two-burn scheme. The first burn is the orbit insertion maneuver, which is performed tangentially to the velocity at periapsis. Thus, the insertion maneuver can be replaced by atmospheric braking (aerocapture) if desired. The second burn is the departure maneuver. Generally, this is a three-dimensional maneuver (i.e., not tangential at periapsis) because the parking orbit and $\boldsymbol{V}_{\infty,D}$ are not perfectly aligned (case 2 of Fig. 1).

However, the departure ΔV can be minimized by proper selection of inclination and departure true anomaly.[7] Because the direction of $\boldsymbol{V}_{\infty,D}$ is included, this departure ΔV will always be greater than or equal to the tangential periapsis ΔV, which only includes the magnitude of $\boldsymbol{V}_{\infty,D}$ [Eq. (1)]. We measure the cost of the two-burn method as this extra ΔV required to account for the direction of $\boldsymbol{V}_{\infty,D}$ (i.e., the two-burn ΔV plus the tangential periapsis ΔV is the total ΔV required to reach the departure trajectory with the two-burn method). Like the apo-twist ΔV, this value provides the additional cost of including the relative geometry between the parking orbit and interplanetary trajectories.

The minimum ΔV and corresponding inclination, using both the apo-twist and two-burn methods, are provided in Tables 1 and 2. The optimal time to perform the apo-twist maneuver for each arrival date is found under the $t_{\Delta V}$ column in these tables. An apo-twist maneuver is generally available at any point in the stay time, but the lowest ΔV maneuvers often occur either at the beginning or end of the stay time. We calculate the heliocentric trajectories by using a point-to-point conic solution between Earth and Mars. The resulting velocities relative to the planet then provide $\boldsymbol{V}_{\infty,A}$ and $\boldsymbol{V}_{\infty,D}$. The ΔV_A and ΔV_D columns give the cost of arriving and departing the orbit with a tangential periapsis burn using Eq. (1). In the case of aerocapture, the propulsive $\Delta V_A = 0$. The ΔV_{add} columns under "apo-twist" and "two-burn" provide the additional cost of achieving the correct direction at departure for these methods. Thus the total cost is

$$\Delta V_{\text{total}} = \Delta V_A + \Delta V_D + \Delta V_{\text{add}} \tag{19}$$

Because the reorientation cost can be a significant fraction of the total ΔV, it cannot be neglected in mission design. Moreover, an economical way of reducing this reorientation ΔV will lower the propellant cost of the mission.

The data in Tables 1 and 2 collectively provide insight into the apo-twist cost and how it compares with the two-burn method. (Similar tables for semicycler and DRM-type missions are provided in Ref. 13.) In addition to the two-burn method, the authors considered several other orbit-coupling techniques (many of which were also examined in Ref. 10), but the two-burn method was found to be the best alternative to the apo-twist.

The apo-twist ΔV is lower than the two-burn ΔV for almost all of the examined missions, which suggests that the apo-twist is more economical than the two-burn method for parking orbits applied to human missions to Mars. Moreover, the inclinations for both methods are similar, and so the two-burn scheme offers no apparent savings for surface rendezvous over the apo-twist. There is no single reason why the two-burn case is sometimes better than the apo-twist (e.g., the 2018 case in Table 2). A modest variation in almost any mission parameter (e.g., parking-orbit period, interplanetary flight time) can change the relative ranking when the two methods are similar in cost. Nevertheless, for an arbitrary mission the apo-twist maneuver is likely to be more efficient than the two-burn method for long-period, eccentric parking orbits. Of course, a scenario that incorporates a rotation at apoapsis (apo-twist) and possible off-periapsis thrusting (two-burn) will provide better performance, but requires more numerical analysis because of the additional degrees of freedom.

If a larger period orbit is used (say, seven days instead of one), then the arrival and departure ΔV decrease, as does the velocity at apoapsis. Because V_{apo} is reduced, the apo-twist ΔV is generally smaller for longer-period orbits. Also, because the velocity at periapsis increases for larger orbits, the average two-burn ΔV rises, countering the effect of using a "loose" parking orbit. In fact, as the parking-orbit period approaches infinity (the parabolic case) the apo-twist ΔV_{add} goes to zero, but the two-burn ΔV_{add} does not. Consequently, increasing the orbit period will almost always decrease the total ΔV with the apo-twist, while the two-burn method can actually gain ΔV. On the other hand, reducing the parking-orbit period increases the probability that the two-burn method will cost less.

One notable drawback to increasing the size of the parking orbit is that there are fewer opportunities to perform the apo-twist maneuver. This effect is more pronounced at Mars than at Earth because the solar and lunar perturbations begin to dominate the decreasing J_2 effects as the size of the orbit increases. In the case where no apo-twist maneuver is available, the apo-twist can be used in conjunction with the two-burn scheme to reduce total mission ΔV. There are also fewer arrival and departure apoapsis crossings if the stay time is relatively short (e.g., one month); however, for long stay times (500–700 days) an apo-twist maneuver is almost always possible.

Figures 7 and 8 provide a sampling of the apo-twist ΔV and departure inclinations for the stop-over cyclers at Mars and Earth, respectively (Tables 1 and 2). In these Figures numerals 1–5 correspond to the five arrival dates in Tables 1 and 2. The arrival inclination is omitted because there is insignificant propellant cost associated with it for aerobraking missions. These figures are particularly useful in examining the trade between ΔV and inclination. For example, arrival date 4 in Fig. 7 has a very low ΔV (0.03 km/s) apo-twist with an inclination of about 140 deg (a retrograde orbit). If a prograde inclination is desired, then an apo-twist with an

Table 1 Stop-over cycler,[4] Mars

		Ideal[a]		Apo-twist				Two-burn	
Arrival date	Stay time, days	ΔV_A, km/s	ΔV_D, km/s	$t_{\Delta V}$, days	i_A, deg	i_D, deg	ΔV_{add}, km/s	i, deg	ΔV_{add}, km/s
7/13/2012	508	1.87	1.53	508	22.2	50.9	0.245	30.1	0.564
8/19/2014	513	1.74	1.01	513	154.8	142.5	0.104	150.8	0.181
10/5/2016	531	1.52	0.82	0	137.6	139.0	0.108	134.5	0.315
10/6/2018	592	2.03	1.38	592	140.5	138.8	0.027	141.7	0.061
2/20/2021	521	0.88	1.63	521	146.1	144.5	0.031	145.7	0.035

[a]For 300-km periapsis altitude and 1-day period orbit.

Table 2 Stop-over cycler,[4] Earth

		Ideal[a]		Apo-twist				Two-burn	
Arrival date	Stay time, days	ΔV_A, km/s	ΔV_D, km/s	$t_{\Delta V}$, days	i_A, deg	i_D, deg	ΔV_{add}, km/s	i, deg	ΔV_{add}, km/s
7/1/2014	617	1.39	1.01	617	30.2	50.2	0.607	36.3	1.273
8/11/2016	637	1.22	0.88	637	140.7	140.4	0.336	136.9	0.795
10/16/2018	648	0.89	1.06	576	119.2	104.4	0.234	115.9	0.141
12/17/2020	640	0.96	1.32	356	117.8	68.5	0.752	94.2	1.698
2/21/2023	615	1.05	1.40	615	26.3	40.3	0.401	33.1	0.979

[a]For 300-km periapsis altitude and 1-day period orbit.

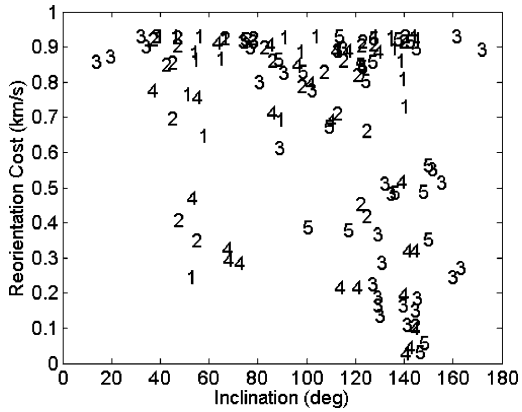

Fig. 7 Apo-twist ΔV vs departure inclination for the five arrival dates in Table 1.

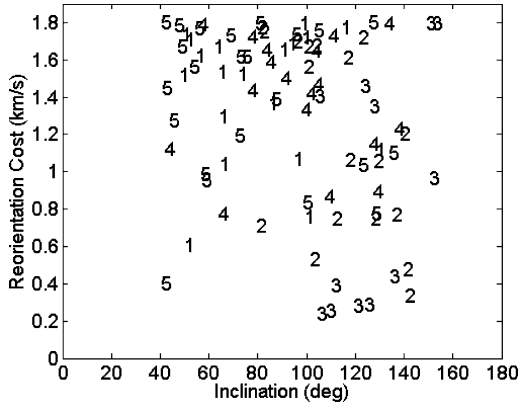

Fig. 8 Apo-twist ΔV vs departure inclination for the five arrival dates in Table 2.

inclination of 40 deg and ΔV of 0.75 km/s is possible for that arrival date. Because there are many different possible apo-twist maneuvers over the stay time (caused by orbital perturbations), there is some freedom in the choice of ΔV, inclination, and maneuver time for a given mission.

We note that arrival dates 1, 2, and 4 in Fig. 7 and dates 1, 2, 4, and 5 in Fig. 8 provide relatively low ΔV apo-twists with prograde departure inclinations (bottom-left quadrant of either graph). Though the ΔV can be higher than the absolute minimum values found in Tables 1 and 2, these maneuvers might be preferred because they reduce the propulsion requirements of the launch vehicle. One way to achieve lower ΔV or a better inclination is to modify the interplanetary trajectories for a more benign $\boldsymbol{V}_\infty$ magnitude or direction. Also, multiple apo-twists can provide an economical means of attaining a desired inclination over the stay time. For example, if the periapsis were targeted to lie in the equatorial plane, an apo-twist at arrival could rotate the trajectory to an equatorial orbit, then another apo-twist at departure would reorient the parking orbit for the return leg. This method could be an interesting extension of the single apo-twist maneuver. Another extension of the apo-twist is the "low-thrust apo-twist," where the orbit would be reoriented over the stay time via low-thrust propulsion (near apoapsis) to allow coapsidal coplanar maneuvers at arrival and departure.

Conclusions

Many Mars mission proposals do not fully account for the geometry between the parking-orbit and the interplanetary trajectories, and thus appreciably underestimate the cost of the mission. An effective way to allow tangential burns at periapsis and still achieve the correct departure direction is to "twist" the orbit about the line of apsides via a maneuver at apoapsis: the apo-twist maneuver. This method works very well for long-period, highly elliptic parking orbits, which are already desired for many proposed missions. We also demonstrate how to harness the natural perturbations on the parking orbit to minimize propellant cost. Reorienting the orbit before departure with the apo-twist almost always requires less ΔV than performing a nontangential maneuver at departure. Consequently, less propellant mass is required, providing a more economical method for the exploration of Mars.

Acknowledgments

The first author's work has been sponsored in part by a Purdue Andrews Fellowship and a National Defense Science and Engineering Graduate Fellowship.

References

[1]Hoffman, S., and Kaplan, D. (eds.), "Human Exploration of Mars: The Reference Mission of the NASA Mars Exploration Study Team," NASA SP-6107, July 1997.

[2]Aldrin, B., Byrnes, D., Jones, R., and Davis, H., "Evolutionary Space Transportation Plan for Mars Cycling Concepts," AIAA Paper 2001-4677, Aug. 2001.

[3]Bishop, R. H., Byrnes, D. V., Newman, D. J., Carr, C. E., and Aldrin, B., "Earth-Mars Transportation Opportunities: Promising Options for Interplanetary Transportation," American Astronautical Society, Paper 00-255, March 2000.

[4]Penzo, P., and Nock, K., "Earth-Mars Transportation Using Stop-Over Cyclers," AIAA Paper 2002-4424, Aug. 2002.

[5]Niehoff, J., Friedlander, A., and McAdams, J., "Earth-Mars Transport Cycler Concepts," International Astronautical Federation, Paper 91-438, Oct. 1991.

[6]Desai, P., Braun, R., and Powell, R., "Aspects of Parking Orbit Selection in a Manned Mars Mission," NASA TP-3256, Dec. 1992.

[7]Desai, P., and Bugulia, J., "Arrival and Departure Impulsive ΔV Determination for Precessing Mars Parking Orbits," *Journal of the Astronautical Sciences*, Vol. 41, No. 1, 1993, pp. 1–18.

[8]Thibodeau, J. R., III, "Use of Planetary Oblateness for Parking-Orbit Alignment," NASA TN D-4657, July 1968.

[9]Desai, P., and Bugulia, J., "Determining Mars Parking Orbits that Ensure Tangential Periapsis Burns at Arrival and Departure," *Journal of Spacecraft and Rockets*, Vol. 30, No. 4, 1993, pp. 414–419.

[10]Luidens, R. W., and Miller, B. A., "Efficient Planetary Parking Orbits with Examples for Mars," NASA TN D-3220, Jan. 1966.

[11]Chao, C. C., "An Analytic Integration of the Averaged Equations of Variation Due to Sun–Moon Perturbations and Its Application," American Astronautical Society, Paper 79-134, June 1979.

[12]Soldner, J. K., "Round Trip Mars Trajectories: New Variations on Classic Mission Profiles," AIAA Paper 90-3794, Aug. 1990.

[13]Landau, D. F., Longuski, J. M., and Penzo, P. A., "Parking Orbits for Human Missions to Mars," American Astronautical Society, AAS Paper 03-514, Aug. 2003.

[14]Cupples, M. L., and Nordwall, J. A., "Optimal Parking Orbits for Manned Mars Missions," American Astronautical Society, Paper 93-149, Feb. 1993.

C. Kluever
Associate Editor